# Mechanisms and Rules of Anion Partition into Ionic Liquids: Phenolate Ions in Ionic Liquid/Water Biphasic Systems

Shoichi Katsuta,* Ko-ichi Nakamura, Yoshihiro Kudo, and Yasuyuki Takeda

Department of Chemistry, Graduate School of Science, Chiba University, 1-33 Yayoi-cho, Inage, Chiba 263-8522, Japan

S *Supporting Information*

ABSTRACT: It is important to understand the mechanisms and general rules of ion partitioning in hydrophobic ionic liquid (IL)/water biphasic systems in order to predict the extractability of an ionic species with various ILs. In this study, we have investigated the partition of picrate ion (target anion, T^-) from aqueous sodium picrate solutions into several ILs and the accompanying changes in aqueous concentrations of the IL component cation (C^+) and anion (A^-) at 298.2 K. The main ILs examined are 1-butyl-3-methylimidazolium bis(trifluoromethanesulfonyl)amide, 1-butyl-3-methylimidazolium hexafluorophosphate, and 1-methyl-3-octylimidazolium bis(trifluoromethanesulfonyl)amide. The aqueous concentrations of C^+ and A^- decreased and increased, respectively, with the extraction of T^- into the IL phase. From the standpoint of equilibrium, the partition behavior of T^- can be explained both by the anion exchange with A^- in the IL phase and by the ion pair extraction with C^+ in the aqueous phase. The aqueous concentrations of C^+ and A^- are governed by the solubility product of the IL (K_{sp}). The distribution ratio of T^- is expressed as a function of $\Delta[T^-]_W$, namely, the difference between the initial and equilibrium concentrations of T^- in the aqueous phase; the distribution ratio of T^- is nearly constant when $\Delta[T^-]_W \ll K_{sp}^{1/2}$, but decreases with increasing $\Delta[T^-]_W$ in the larger $\Delta[T^-]_W$ region. The equilibrium constants of the ion pair extraction and the ion exchange extraction have been determined for picrate and other phenolate ions whose partition data were previously reported. The dependences of the extraction constants and extractability on the kinds of IL component ions can be quantitatively explained on the basis of the variations of K_{sp}.
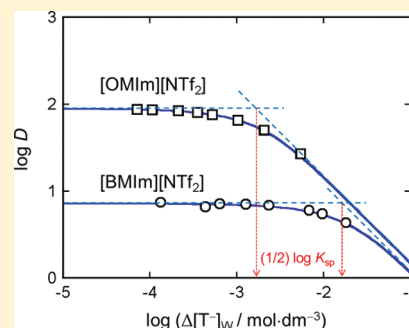
■ INTRODUCTION

Room temperature ionic liquids (ILs) have attracted much attention as green solvents owing to their nonvolatility which assures nonflammability and, in general, a low impact on the environment and human health. There is an increasing need for the use of ILs as alternatives to conventional organic solvents in a number of chemical fields, including analytical and separation chemistry.[1−6] As described in recent reviews,[7−13] one of the important applications of ILs is the use in liquid−liquid extraction. Hydrophobic ILs have potential as novel extraction media for various chemical substances such as small organic compounds, biological compounds, and metals. The solute partition coefficient is a key parameter determining the extraction performance. In a previous work,[14] the partition coefficients of various chlorophenols and nitrophenols were determined in some IL/water biphasic systems and considerably high extractabilities were observed for their anionic forms (phenolate ions). It is a characteristic property of the ILs that they can extract ionic species from aqueous solutions without the aid of additional counterions such as ion-pairing agents. In addition, the extractability of each phenolate ion was found to be much more dependent on the kind of IL than the extractability of its conjugate acid (neutral phenol). There are virtually unlimited number of possible ionic liquids by different cation/anion combinations; therefore, it is important to understand the mechanisms and general rules of the ion partitioning in IL/water biphasic systems.

When a monovalent target anion (T^-) is transferred from water into a hydrophobic IL which is composed of a cation (C^+) and an anion (A^-), the following two mechanisms can be considered on the basis of the electroneutrality principle:

ion pair extraction :
$$T_W^- + C_W^+ \rightarrow T_{IL}^- + C_{IL}^+ \tag{1}$$
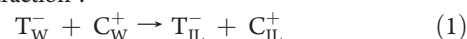
ion exchange extraction :
$$T_W^- + A_{IL}^- \rightarrow T_{IL}^- + A_w^- \tag{2}$$
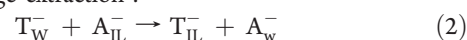
Here, subscripts "W" and "IL" denote the aqueous and IL phases, respectively. The ion pair extraction (eq 1) is a mechanism similar to that generally observed in a conventional organic solvent/water system in the presence of a hydrophobic cation. On the other hand, the ion exchange extraction (eq 2), which was first proposed by Dietz et al. for the cation extraction with ILs,[15] is widely accepted as a main mechanism in an IL/water system.[16−20] The transfer of simple ions from water to a few ILs was also studied on the basis of the standard ion-transfer potentials from the electrochemical point of view.[21−23] However, the factors governing the ion partition in IL/water systems have not been sufficiently established as compared to conventional organic solvent/water systems.

ACS Publications   © 2011 American Chemical Society

852

dx.doi.org/10.1021/jp210444n | *J. Phys. Chem. B* 2012, 116, 852–859

This paper reports the mechanisms and rules found for the partition of picrate (2,4,6-trinitrophenolate) anion from water to several hydrophobic ILs at 298.2 K. The reason for using picrate as a model anion is that this anion is chemically stable, is hard to be protonated, and has both high extractability and high visible-light absorption which allow us to easily measure the distribution ratio in the IL/water systems. The concentrations of the IL component cation and anion in the aqueous phase were also measured. The hydrophobic ILs used were 1-butyl-3-methylimidazolium bis(trifluoromethanesulfonyl)amide ($[BMIm][NTf_2]$), 1-butyl-3-methylimidazolium hexafluorophosphate ($[BMIm][PF_6]$), 1-methyl-3-octylimidazolium bis(trifluoromethanesulfonyl)amide ($[OMIm][NTf_2]$), 1-methyl-3-octylimidazolium tetrafluoroborate ($[OMIm][BF_4]$), and 1-butyl-1-methylpyrrolidinium bis(trifluoromethanesulfonyl)amide ($[BMPyr][NTf_2]$). The salts of $[BF_4]^-$ and $[PF_6]^-$ are not always "green" because they can be hydrolyzed, producing hydrogen fluoride; however, we used them because the data of these common ionic liquids are valuable for the fundamental study. The findings are applied to the partition of other phenolate ions whose experimental data were reported previously.[14]

■ EXPERIMENTAL SECTION

Materials. Special grade reagents of $[BMIm][NTf_2]$ (impurities H_2O, 10 ppm; Li^+, 0.2 ppm; Na^+, 0.1 ppm; F^-, 10 ppm; Cl^-, 10 ppm) and $[BMPyr][NTf_2]$ (impurities H_2O, 3 ppm; Li^+, < 0.2 ppm; Na^+, < 0.1 ppm; F^-, 1 ppm; Cl^-, 1 ppm) were supplied from Kanto Chemical Co. (Tokyo, Japan) and used without further purification. $[BMIm][PF_6]$ (high purity grade), $[OMIm][NTf_2]$ (high purity grade), and $[OMIm][BF_4]$ (for synthesis grade) were purchased from Merck (Darmstadt, Germany); they were washed three times with deionized water just prior to use. Water was distilled and further deionized with a Milli-Q Lab system (Millipore, Billerica, MA). Dichloromethane and chloroform of guaranteed reagent grade (Kanto Chemical Co.) were washed three times with deionized water prior to use. Sodium picrate monohydrate ($Na[Pic]\cdot H_2O$) of extra-pure reagent grade (Kanto Chemical Co.), lithium bis(trifluoromethanesulfonyl)amide ($Li[NTf_2]$) of "for advanced material research" grade (Kanto Chemical Co.), and lithium hexafluorophosphate ($Li[PF_6]$) of 97.0% purity (Tokyo Chemical Industry Co., Tokyo, Japan) were used without further purification. Other reagents were of guaranteed reagent grade and used as obtained.

Partition Experiments. An aqueous solution of $Na[Pic]$ (7.9×10^{-5} to 2.6×10^{-2} mol·dm^{-3}) and a water-saturated IL ($[BMIm][NTf_2]$, $[BMIm][PF_6]$, or $[OMIm][NTf_2]$) were placed in a stoppered glass tube. Here, the volume of the viscous IL phase was accurately evaluated from the mass by using the densities of the water-saturated ILs; 1.4311 g·cm^{-3} for $[BMIm]$-$[NTf_2]$,[24] 1.3550 g·cm^{-3} for $[BMIm][PF_6]$,[24] and 1.3276 g·cm^{-3} for $[OMIm][NTf_2]$.[14] The volume ratio of the IL phase to the aqueous phase was adjusted to 1/2, 3/2, and 1/10 for $[BMIm][NTf_2]$, $[BMIm][PF_6]$, and $[OMIm][NTf_2]$, respectively; in these cases, the loss of the ILs upon their dissolution into the aqueous phase was expected to be less than 1% from the solubility data (Table 1). When the IL phase was $[BMIm][NTf_2]$ or $[BMIm][PF_6]$, an aqueous solution containing both $Na[Pic]$ and $Li[NTf_2]$ (8.6×10^{-3} to 1.7×10^{-2} mol·dm^{-3}) or $Li[PF_6]$ (3.7×10^{-2} mol·dm^{-3}) was also used, respectively. The biphasic mixture in the glass tube was equilibrated by stirring with a magnetic stirrer for 1 h in a water bath thermostated at 298.2 ± 0.2 K. The two phases were completely separated by centrifugation, and the glass

Table 1. Solubilities and Solubility Products (K_{sp})^a of Ionic Liquids in Water at 298.2 K

IL	solubility/mol·dm^{-3}	$K_{sp}/(\text{mol·dm}^{-3})^2$
$[BMIm][NTf_2]$	$(1.643 \pm 0.008) \times 10^{-2}$	2.70×10^{-4}
	$1.70 \times 10^{-2 b}$	
$[BMIm][PF_6]$	$(7.36 \pm 0.04) \times 10^{-2}$	5.42×10^{-3}
	$6.70 \times 10^{-2, c}$ $7.14 \times 10^{-2 d}$	
$[OMIm][NTf_2]$	$(1.66 \pm 0.03) \times 10^{-3}$	2.76×10^{-6}
	$1.86 \times 10^{-3, b}$ $1.55 \times 10^{-3 e}$	
$[OMIm][BF_4]$	$(6.2 \pm 0.1) \times 10^{-2}$	3.8×10^{-3}
	$6.48 \times 10^{-2 d}$	
$[BMPyr][NTf_2]$	$(1.49 \pm 0.03) \times 10^{-2}$	2.22×10^{-4}

^{a} Calculated as the square of solubility. ^{b} Ref 25. ^{c} Ref 26. ^{d} Ref 27 (295 K). ^{e} Ref 28.

tube was allowed to stand for more than 15 min in the thermostated water bath. The concentration of $[Pic]^-$ in the aqueous phase was determined spectrophotometrically ($\lambda_{max} = 356.0$ nm, $\varepsilon = (1.45 \pm 0.01) \times 10^4$ cm^{-1}·mol^{-1}·dm^3). The concentration of $[Pic]^-$ in the IL phase was calculated based on the mass balance, and the distribution ratio (D) was calculated as the ratio of the molar concentration in the IL phase to that in the aqueous phase. In order to evaluate the partition of Na^+ and Li^+ into the IL phase, the IL phase was washed with deionized water and the concentrations of the alkali metals in the washing water were measured by atomic absorption spectrophotometry with hollow cathode lamps; their concentrations were found to be negligibly small.

The aqueous concentration of the IL cation ($[BMIm]^+$ or $[OMIm]^+$) were determined as follows. An aliquot of the aqueous phase was transferred into another stoppered glass tube, to which $Na[Pic]$ and $NaOH$ were added so that their concentrations became 5×10^{-2} and 1×10^{-3} mol·dm^{-3}, respectively. Dichloromethane, whose volume was equal to that of the aqueous solution, was further added, and the biphasic mixture was stirred for 30 min. It was confirmed that the IL cation in the aqueous phase was quantitatively extracted as an ion pair with $[Pic]^-$ into the dichloromethane phase. The concentration in the dichloromethane phase was determined spectrophotometrically ($\lambda_{max} = 367.8$ nm, $\varepsilon = (1.70 \pm 0.04) \times 10^4$ cm^{-1}·mol^{-1}·dm^3 for $[BMIm]^+$; $\lambda_{max} = 367.8$ nm, $(1.72 \pm 0.02) \times 10^4$ cm^{-1}·mol^{-1}·dm^3 for $[OMIm]^+$).

For the $[BMIm][NTf_2]$ system, the aqueous concentration of the IL anion ($[NTf_2]^-$) was determined as follows. An aliquot of the aqueous phase was transferred into another stoppered glass tube, to which methylene blue and NaH_2PO_4 were added so that their concentrations became 8×10^{-4} and 8×10^{-1} mol·dm^{-3}, respectively. Chloroform, whose volume was equal to that of the aqueous solution, was further added, and the biphasic mixture was stirred for 1 h. By this operation, both $[NTf_2]^-$ and $[Pic]^-$ in the aqueous phase were quantitatively extracted as ion pairs with methylene blue into the chloroform phase. The absorbance at 652.0 nm of the chloroform phase was measured. The absorbance measured was the sum of the absorbance for the methylene blue salts of $[NTf_2]^-$ and $[Pic]^-$; the concentration of $[NTf_2]^-$ was calculated by considering the contribution of $[Pic]^-$ ($\lambda_{max} = 652.0$ nm, $\varepsilon = (1.20 \pm 0.03) \times 10^5$ cm^{-1}·mol^{-1}·dm^3 for $[NTf_2]^-$; $\lambda_{max} = 652.0$ nm, $(1.06 \pm 0.04) \times 10^5$ cm^{-1}·mol^{-1}·dm^3 for $[Pic]^-$).

Solubilities of ILs in Water. The solubilities of $[BMIm]$-$[NTf_2]$, $[BMIm][PF_6]$, $[OMIm][NTf_2]$, $[OMIm][BF_4]$, and $[BMPyr][NTf_2]$ in water were determined by measuring the

Table 2. Concentrations of $[BMIm]^+$, $[NTf_2]^-$, and $[Pic]^-$ in the Aqueous Phase and Distribution Ratio of $[Pic]^-$ for $[BMIm][NTf_2]/H_2O$ System[a] at 298.2 K

	init concn in the aq phase/ mmol·dm^{-3}		equilib concn in the aq phase/ mmol·dm^{-3}			
no.	Na[Pic]	Li[NTf$_2$]	[BMIm]$^+$	[NTf$_2$]$^-$	[Pic]$^-$	log D
1	0.168	17.2	10.4	26.8	0.0503	0.663
2	0.168	8.61	12.9	21.0	0.0433	0.759
3	0.168	0	16.5	16.6	0.0354	0.873
4	0.565	0	16.5	16.4[b]	0.131	0.820
5	0.807	0	16.4	16.4[b]	0.176	0.857
6	1.61	0	16.0	16.9[b]	0.355	0.852
7	2.99	0	15.7	17.2[b]	0.671	0.840
8	8.97	0	13.6	19.9[b]	2.23	0.782
9	13.1	0	12.6	20.5	3.48	0.742
10	26.2	0	10.5	25.9	8.25	0.639

[a] The volume ratio of the ionic liquid phase to the aqueous phase is 1/2.
[b] Calculated from the K_{sp} value of $[BMIm][NTf_2]$ and the concentration of $[BMIm]^+$.

Table 3. Concentrations of $[BMIm]^+$, $[PF_6]^-$, and $[Pic]^-$ in the Aqueous Phase and Distribution Ratio of $[Pic]^-$ for $[BMIm][PF_6]/Water$ System[a] at 298.2 K

	init concn in the aq phase/ mmol·dm^{-3}		equilib concn in the aq phase/ mmol·dm^{-3}			
no.	Na[Pic]	Li[PF$_6$]	[BMIm]$^+$	[PF$_6$]$^{-b}$	[Pic]$^-$	log D
1	0.524	36.9	57.5	94.2	0.0116	1.469
2	0.524	0	70.8	76.6	0.00945	1.560
3	26.2	0	64.4	84.2	0.521	1.517

[a] The volume ratio of the ionic liquid phase to the aqueous phase is 3/2.
[b] Calculated from the K_{sp} value of $[BMIm][PF_6]$ and the concentration of $[BMIm]^+$.

Table 4. Concentrations of $[OMIm]^+$, $[NTf_2]^-$, and $[Pic]^-$ in the Aqueous Phase and Distribution Ratio of $[Pic]^-$ for $[OMIm][NTf_2]/Water$ System[a] at 298.2 K

	init concn in the aq phase/mmol·dm^{-3}	equilib concn in the aq phase/mmol·dm^{-3}			
no.	Na[Pic]	[OMIm]$^+$	[NTf$_2$]$^{-b}$	[Pic]$^-$	log D
1	0.0792	1.61	1.71	0.00817	1.939
2	0.119	1.59	1.74	0.0124	1.932
3	0.237	1.55	1.78	0.0253	1.924
4	0.396	1.48	1.86	0.0438	1.905
5	0.594	1.41	1.96	0.0695	1.878
6	1.19	1.20	2.30	0.158	1.815
7	2.48	0.927	2.98	0.413	1.700
8	7.44	0.519	5.32	2.01	1.431

[a] The volume ratio of the ionic liquid phase to the aqueous phase is 1/10.
[b] Calculated from the K_{sp} value of $[OMIm][NTf_2]$ and the concentration of $[OMIm]^+$.

cation concentrations in aqueous solutions saturated with the ILs at 298.2 ± 0.2 K by the above-mentioned method using Na[Pic], where the data of λ_{max} and ε for $[BMPyr]^+$ are 374.8 nm and $(1.69 \pm 0.04) \times 10^4$ cm^{-1}·mol^{-1}·dm^3, respectively. The solubility product (K_{sp}) of an IL in water was calculated as the product of the molar concentrations of the IL cation and anion in the IL-saturated water, assuming the activity coefficients to be unity and neglecting any ion association. The values of the solubility and the solubility product are summarized in Table 1, together with the literature values of the solubility.[25−28] The solubility values obtained in this study are generally in agreement with the literature values, considering the discrepancy of the published data from different sources.

■ RESULTS AND DISCUSSION

Concentrations of IL Component Ions. For the $[BMIm][NTf_2]/water$ system, the equilibrium concentrations of $[Pic]^-$, $[BMIm]^+$, and $[NTf_2]^-$ in the aqueous phase are listed in Table 2, together with the initial composition of the aqueous phase. Formation of ion associates such as $[BMIm]^+[NTf_2]^-$ and $[BMIm]^+[Pic]^-$ in the aqueous phase can be neglected by considering small values of the association constants reported previously.[29] The results obtained with different initial concentrations of Na[Pic] (data no. 3, 9, and 10 in Table 2) show that the equilibrium concentrations of the IL component ions, $[[BMIm]^+]_W$ and $[[NTf_2]^-]_W$, decreased and increased, respectively, with an increase of the initial concentration of Na[Pic]. It is expected from the results in the presence of Li[NTf$_2$] (data no. 1 and 2 in Table 2) that an increase of $[[NTf_2]^-]_W$ is responsible for a decrease of $[[BMIm]^+]_W$. In addition, the value of $[[BMIm]^+]_W \times [[NTf_2]^-]_W$ is always constant, i.e., $(2.71 \pm 0.08) \times 10^{-4}$ mol^2·dm^{-6}, which is in good agreement with the solubility product of $[BMIm][NTf_2]$ in water, 2.70×10^{-4} mol^2·dm^{-6} (Table 1). Therefore, it is experimentally proved that the following solubility product relationship holds for the ionic liquid component ions in the aqueous phase.

$$K_{sp} = [C^+]_W[A^-]_W \qquad (3)$$

The $[[NTf_2]^-]_W$ values for data no. 4−8 in Table 2 were calculated from the solubility product and the measured values of $[[BMIm]^+]_W$. For the $[BMIm][PF_6]/water$ and $[OMIm][NTf_2]/water$ systems, the equilibrium concentrations of the IL anions in the aqueous phase were all calculated assuming the solubility product relationship; the results are summarized in Tables 3 and 4.

Theory of Anion Extraction with ILs. As shown in Table 2, the distribution ratio of $[Pic]^-$ in the $[BMIm][NTf_2]/water$ system was not dependent on the initial concentration of Na[Pic] when the concentration was less than 3×10^{-3} mol·dm^{-3} (data no. 3−7), whereas it decreased with increasing initial Na[Pic] concentration when the concentration was higher (data no. 8−10). The distribution ratio of $[Pic]^-$ decreased also with the addition of Li[NTf$_2$] (data no. 1 and 2). Similar results were observed in the $[BMIm][PF_6]/water$ and $[OMIm][NTf_2]/water$ systems (Tables 3 and 4, respectively).
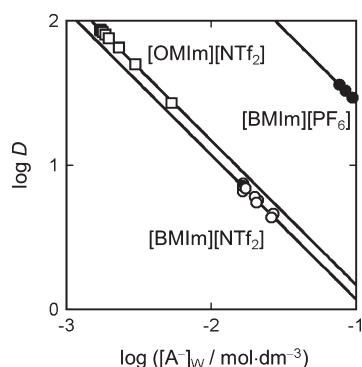
Supposing that the target anion T^- is extracted by ion pair extraction (eq 1) or ion exchange (eq 2), the following equations are derived.

$$\log D = \log K_{IP-ex} + \log[C^+]_W \qquad (4)$$

$$\log D = \log K_{IE-ex} - \log[A^-]_W \qquad (5)$$
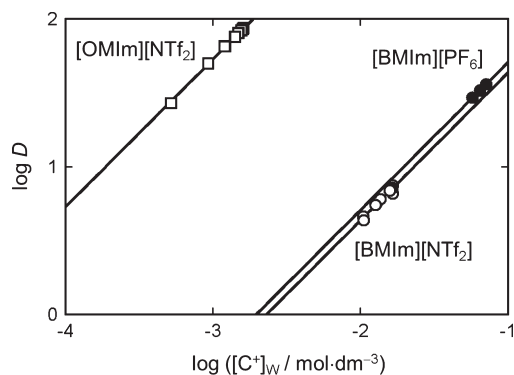
Figure 1. Relationship between logarithmic values of the distribution ratio of $[Pic]^-$ and of the aqueous concentration of IL cation at equilibrium. The solid lines are regression lines based on eq 4.

Figure 2. Relationship between logarithmic values of the distribution ratio of $[Pic]^-$ and of the aqueous concentration of IL anion at equilibrium. The solid lines are regression lines based on eq 5.

Here, K_{IP-ex} and K_{IE-ex} are the equilibrium constants for the ion pair extraction and the ion exchange extraction, respectively.

$$K_{IP-ex} = [T^-]_{IL}/[T^-]_W[C^+]_W \tag{6}$$

$$K_{IE-ex} = [T^-]_{IL}[A^-]_W/[T^-]_W \tag{7}$$

These equations are based on the assumption of dilute solutions. Therefore, with regard to C^+ and A^- in the aqueous phase and T^- in both the phases, it is assumed that their activity coefficients are unity and no aggregates or micelles are formed. The concentrations of C^+ and A^- in the IL phase are not included on the right side of eqs 6 and 7 because their activities are regarded as constant. The $[T^-]_{IL}$ term, denoting the concentration of T^- in the IL phase, is used regardless of the state (free anion or ion pair with C^+). In Figures 1 and 2, the log D values of $[Pic]^-$ in the $[BMIm][NTf_2]$/water, $[BMIm][PF_6]$/water, and $[OMIm][NTf_2]$/water systems are plotted against the log $[C^+]_W$ and log $[A^-]_W$ values, respectively. Interestingly, both the plots of Figures 1 and 2 for a given system show linear relationships as expected from eqs 4 and 5. The values of K_{IP-ex} and K_{IE-ex} are summarized in Tables 5 and 6, respectively. Therefore, from the standpoint of equilibrium, the extraction of Pic^- can be explained by both the chemical reactions of ion pair extraction (eq 1) and ion exchange (eq 2). The reason for the relations of eqs 4 and 5 holding simultaneously lies in the fact that the solubility product relationship (eq 3) holds for $[C^+]_W$ and

$[A^-]_W$ in the aqueous phase. Equations 6 and 7 lead to the following relationship.

$$K_{IE-ex}/K_{IP-ex} = K_{sp} \tag{8}$$

This relationship should hold regardless of the kind of extracted ion.

The following equation is given from the charge balance in the aqueous phase.

$$[T^-]_W{}^0 - [T^-]_W = [A^-]_W - [C^+]_W \tag{9}$$

Here, $[T^-]_W{}^0$ denotes the initial concentration of T^- in the aqueous phase, which equals the initial concentration of $Na[Pic]$ and also $[Na^+]_W$ in the present study. Introducing the relationship of eq 3 into eq 9, the following two equations are given.

$$[T^-]_W{}^0 - [T^-]_W = K_{sp}/[C^+]_W - [C^+]_W \tag{10}$$

$$[T^-]_W{}^0 - [T^-]_W = [A^-]_W - K_{sp}/[A^-]_W \tag{11}$$

Equations 10 and 11 are quadratic equations of $[C^+]_W$ and $[A^-]_W$, respectively. Therefore, when $([T^-]_W{}^0 - [T^-]_W)$ is represented by $\Delta[T^-]_W$, the concentrations $[C^+]_W$ and $[A^-]_W$ are expressed as follows:

$$[C^+]_W = \{-\Delta[T^-]_W + (\Delta[T^-]_W{}^2 + 4K_{sp})^{1/2}\}/2 \tag{12}$$

$$[A^-]_W = \{\Delta[T^-]_W + (\Delta[T^-]_W{}^2 + 4K_{sp})^{1/2}\}/2 \tag{13}$$

These equations indicate that $[C^+]_W$ and $[A^-]_W$ are functions of $\Delta[T^-]_W$. The log $[C^+]_W$ and log $[A^-]_W$ values determined experimentally are plotted against log $\Delta[T^-]_W$ in Figure 3. The solid lines in Figure 3 are theoretical curves from eqs 12 and 13, which are in good agreement with the experimental results.

Substituting $[C^+]_W$ and $[A^-]_W$ in eqs 4 and 5 by eqs 12 and 13, respectively, the following equations are obtained.

$$\log D = \log K_{IP-ex} + \log\{-\Delta[T^-]_W + (\Delta[T^-]_W{}^2 + 4K_{sp})^{1/2}\} - \log 2 \tag{14}$$

$$\log D = \log K_{IE-ex} - \log\{\Delta[T^-]_W + (\Delta[T^-]_W{}^2 + 4K_{sp})^{1/2}\} + \log 2 \tag{15}$$

Equations 14 and 15 are essentially identical to each other. The asymptotic line when $\Delta[T^-]_W \to \infty$ and that when $\Delta[T^-]_W \to 0$ are as follows:

$$\Delta[T^-]_W \to \infty :$$

$$\log D = \log K_{IP-ex} + \log K_{sp} - \log \Delta[T^-]_W$$
$$= \log K_{IE-ex} - \log \Delta[T^-]_W \tag{16}$$

$$\Delta[T^-]_W \to 0 :$$

$$\log D = \log K_{IE-ex} - (1/2)\log K_{sp}$$
$$= \log K_{IP-ex} + (1/2)\log K_{sp} \tag{17}$$

According to eq 16, the distribution ratio of T^- varies in inverse proportion to $\Delta[T^-]_W$. On the other hand, eq 17 indicates that

Table 5. Equilibrium Constants for Phenolates in Ion Pair Extraction from Water to Ionic Liquid at 298.2 K[a]

no.	solute	IL = [BMIm][NTf$_2$]	[BMPyr][NTf$_2$]	[BMIm][PF$_6$]	[OMIm][NTf$_2$]	[OMIm][BF$_4$]
			log $(K_{IP\text{-}ex}/\text{mol}^{-1}\cdot\text{dm}^3)$			
1	phenolate					1.48
2	2-chlorophenolate	−0.34	0.26	−0.25		2.37
3	3-chlorophenolate	0.52	0.37	0.80		
4	4-chlorophenolate	1.01	1.19	0.60		2.55
5	2,3-dichlorophenolate	0.37	0.35	0.39		3.28
6	3,5-dichlorophenolate	0.51	0.61	0.65		3.48
7	2,4,6-trichlorophenolate	1.47		1.22		4.06
8	pentachlorophenolate	2.69		2.57		
9	2-nitrophenolate			0.65	2.40	2.90
10	3-nitrophenolate			0.22		2.58
11	4-nitrophenolate			0.77		
12	2,4-dinitrophenolate	1.49	1.43	1.45	3.20	3.96
13	2,6-dinitrophenolate	1.50	1.35	1.53		
14	picrate	2.70	2.62	2.69	4.71	4.95
		2.64 ± 0.02[b]		2.709 ± 0.001[b]	4.73 ± 0.01[b]	

[a] Most of the values are calculated from the partition data reported in ref 14 using eq 19. [b] Calculated from the partition data obtained in this study using eq 4.

Table 6. Equilibrium Constants for Phenolates in Ion Exchange Extraction from Water to Ionic Liquid at 298.2 K[a]

no.	solute	IL = [BMIm][NTf$_2$]	[BMPyr][NTf$_2$]	[BMIm][PF$_6$]	[OMIm][NTf$_2$]	[OMIm][BF$_4$]
			log $(K_{IE\text{-}ex}/\text{mol}\cdot\text{dm}^{-3})$			
1	phenolate					−0.91
2	2-chlorophenolate	−3.90	−3.40	−2.51		−0.05
3	3-chlorophenolate	−3.04	−3.29	−1.46		
4	4-chlorophenolate	−2.55	−2.47	−1.66		0.13
5	2,3-dichlorophenolate	−3.19	−3.31	−1.87		0.86
6	3,5-dichlorophenolate	−3.05	−3.05	−1.61		1.06
7	2,4,6-trichlorophenolate	−2.09		−1.04		1.64
8	pentachlorophenolate	−0.87		0.31		
9	2-nitrophenolate			−1.61	−3.16	0.48
10	3-nitrophenolate			−2.04		0.16
11	4-nitrophenolate			−1.49		
12	2,4-dinitrophenolate	−2.07	−2.23	−0.81	−2.36	1.54
13	2,6-dinitrophenolate	−2.06	−2.31	−0.73		
14	picrate	−0.87	−1.04	0.43	−0.85	2.53
		−0.93 ± 0.02[b]		0.443 ± 0.001[b]	−0.83 ± 0.01[b]	

[a] Most of the values are calculated from the partition data reported in ref 14 using eq 20. [b] Calculated from the partition data obtained in this study using eq 5.

the distribution ratio of T$^-$ is constant, regardless of the value of $\Delta[\text{T}^-]_W$. The $\log \Delta[\text{T}^-]_W$ value at the intersection point of these asymptotic lines equals to $(1/2)\log K_{sp}$. Therefore, the $\Delta[\text{T}^-]_W$ dependence of the distribution ratio of T$^-$ changes around $\Delta[\text{T}^-]_W = K_{sp}^{1/2}$, namely, the aqueous solubility of IL. In Figure 4, the $\log D$ values of $[\text{Pic}]^-$ (T$^-$) in the [BMIm][NTf$_2$]/water and [OMIm][NTf$_2$]/water systems are plotted against the $\log \Delta[\text{T}^-]_W$ value. The solid lines in the figure are calculated from eq 14 or 15. The broken lines are the asymptotic lines from eqs 16 and 17, and the $(1/2)\log K_{sp}$ values are −1.784 and −2.780 for [BMIm][NTf$_2$] and [OMIm][NTf$_2$], respectively. The agreement between the

experimental results and the theoretical predictions is quite satisfactory.

If no T$^-$ is extracted, the aqueous concentrations of C$^+$ and A$^-$ are both equal to $K_{sp}^{1/2}$. As described in the above discussion, IL extracts T$^-$ by increasing the aqueous concentration of A$^-$ and decreasing that of C$^+$. Therefore, the increase of the aqueous A$^-$ concentration from $K_{sp}^{1/2}$ corresponds to the amount of T$^-$ extracted by the ion exchange mechanism (eq 2), whereas the decrease of the aqueous C$^+$ concentration from $K_{sp}^{1/2}$ corresponds to the amount of T$^-$ extracted by the ion pair mechanism (eq 1). For example, the contribution of the ion exchange mechanism in the total extraction, $R_{IE}(\%)$, can be evaluated by
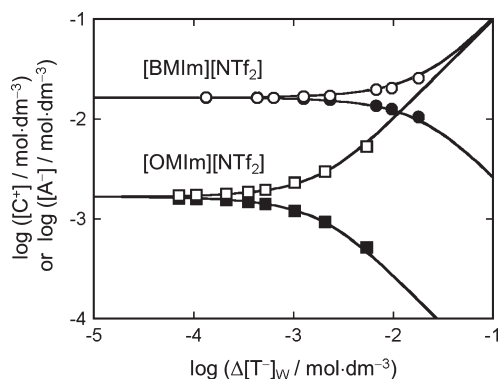
Figure 3. Aqueous concentrations of IL cation (filled symbols) and IL anion (open symbols) as a function of the difference between the initial and equilibrium concentrations of $[Pic]^-$ in the aqueous phase. The solid lines are calculated results from eqs 12 and 13.
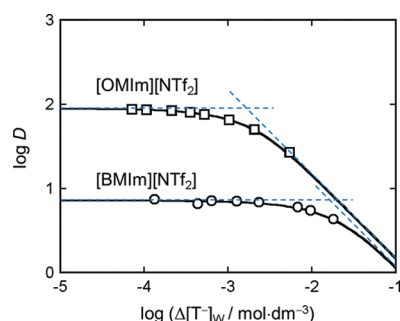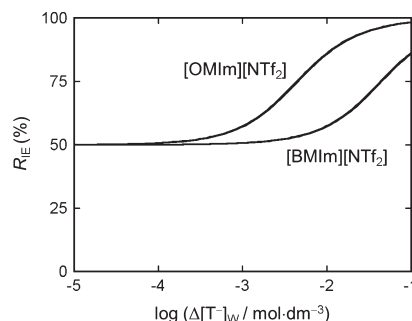

Figure 4. Distribution ratio of $[Pic]^-$ as a function of the difference between the initial and equilibrium concentrations of $[Pic]^-$ in the aqueous phase. The solid lines are calculated results from eq 14 or eq 15. The broken lines are the asymptotic lines from eqs 16 and 17.

the following equation.

$$
\begin{aligned}
R_{IE}(\%) &= 100([A^-]_W - K_{sp}^{1/2})/([T^-]_W^{\ 0} - [T^-]_W) \\
&= 100[\{\Delta[T^-]_w + (\Delta[T^-]_w^{\ 2} + 4K_{sp})^{1/2}\}/2 \\
&\quad - K_{sp}^{1/2}]/\Delta[T^-]_w \\
&= 100[1/2 + \{(1/2)^2 \\
&\quad + (K_{sp}^{1/2}/\Delta[T^-]_W)^2\}^{1/2} - K_{sp}^{1/2}/\Delta[T^-]_W] \quad (18)
\end{aligned}
$$

In Figure 5, the $R_{IE}(\%)$ values calculated from eq 18 are shown as a function of $\log \Delta[T^-]_W$ for the $[BMIm][NTf_2]$/water and $[OMIm][NTf_2]$/water systems. When the $\Delta[T^-]_W$ value is sufficiently small compared with $K_{sp}^{1/2}$, the $R_{IE}(\%)$ value is nearly 50% (never less than 50%). In this case, the contribution of the ion exchange extraction is nearly equal to that of the ion pair one. When the $\Delta[T^-]_W$ value becomes around $K_{sp}^{1/2}$, the $R_{IE}(\%)$ value increases with increasing $\Delta[T^-]_W$. In the region when the $\Delta[T^-]_W$ value is greater than $K_{sp}^{1/2}$, the contribution of the ion exchange extraction is dominant.

Extraction Equilibrium Constants of ILs for Phenolate Anions. In a previous paper,[14] we reported the partition coefficients of various chlorinated and nitrated phenolate ions in several IL/water systems. The partition coefficients correspond to the distribution ratio determined in this study. Since the partition data were all obtained under the condition that $\Delta[T^-]_W \ll K_{sp}^{1/2}$, the K_{IP-ex} and K_{IE-ex} values can be calculated by the following

Figure 5. Contribution of the ion exchange mechanism in the total extraction of $[Pic]^-$ as a function of the difference between the initial and equilibrium concentrations of $[Pic]^-$ in the aqueous phase (calculated results from eq 18).

equations which are derived from eqs 4 and 5 by substituting $[C^+]_W$ and $[A^-]_W$ with $K_{sp}^{1/2}$.

$$\log K_{IP-ex} = \log D - (1/2)\log K_{sp} \quad (19)$$

$$\log K_{IE-ex} = \log D + (1/2)\log K_{sp} \quad (20)$$

The K_{IP-ex} and K_{IE-ex} values obtained are summarized in Tables 5 and 6, respectively, together with the values for $[Pic]^-$.

For a given phenolate ion, the K_{IP-ex} values for $[BMPyr][NTf_2]$, $[BMIm][NTf_2]$, and $[BMIm][PF_6]$ are generally similar to each other. Compared with them, $[OMIm][NTf_2]$ and $[OMIm][BF_4]$ have much larger K_{IP-ex} values. The K_{IP-ex} value of $[OMIm][BF_4]$ is somewhat larger than that of $[OMIm][NTf_2]$. Therefore, the ion pair extraction power of the ILs toward the phenolate anions is much more dependent on the component cation than on the component anion. On the other hand, the K_{IE-ex} value for a given phenolate anion changes little with the component cation among $[BMIm][NTf_2]$, $[BMPyr][NTf_2]$, and $[OMIm][NTf_2]$, but depends largely on the component anion as follows: $[BMIm][NTf_2] < [BMIm][PF_6]$ and $[OMIm][NTf_2] \ll [OMIm][BF_4]$. As expected from the chemical equations (eqs 1 and 2), a greater K_{IP-ex} value is observed for a more bulky (more hydrophobic) component cation, whereas a greater K_{IE-ex} value for a less bulky (more hydrophilic) anion.

Using the standard Gibbs energies of single ion transfer from the aqueous phase to the IL phase ($\Delta G^\circ_{tr,W\to IL}$), the standard Gibbs energy of ion pair extraction ($\Delta G^\circ_{IP-ex} = -RT \ln K_{IP-ex}$) and that of ion exchange extraction ($\Delta G^\circ_{IE-ex} = -RT \ln K_{IE-ex}$) can be expressed as follows:

$$\Delta G^\circ_{IP-ex} = \Delta G^\circ_{tr,w\to IL}(T^-) + \Delta G^\circ_{tr,w\to IL}(C^+) \quad (21)$$

$$\Delta G^\circ_{IE-ex} = \Delta G^\circ_{tr,w\to IL}(T^-) - \Delta G^\circ_{tr,w\to IL}(A^-) \quad (22)$$

On the other hand, the standard Gibbs energy of dissolution of IL in water ($\Delta G^\circ_{s,W} = -RT \ln K_{sp}$) is expressed as follows:

$$\Delta G^\circ_{s,W} = -\Delta G^\circ_{tr,w\to IL}(C^+) - \Delta G^\circ_{tr,w\to IL}(A^-) \quad (23)$$

Therefore, the following equations are derived.

$$\Delta G^\circ_{IP-ex} = \Delta G^\circ_{tr,W\to IL}(T^-) - \Delta G^\circ_{tr,W\to IL}(A^-) - \Delta G^\circ_{s,W} \quad (24)$$
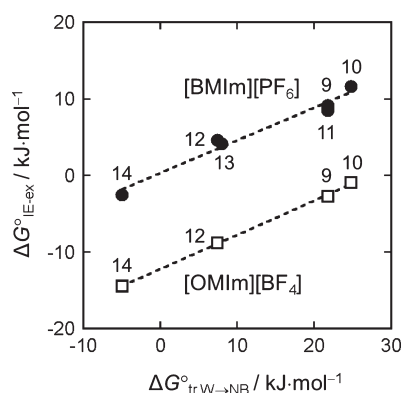
Figure 6. Correlation between the standard Gibbs energy of ion exchange extraction for phenolate ions from water to IL and that of their transfer from water to nitrobenzene. The numbers of solutes (phenolates) correspond to those in Tables 5 and 6.

$$\Delta G^\circ_{\text{IE-ex}} = \Delta G^\circ_{\text{tr},w \to \text{IL}}(\text{T}^-) + \Delta G^\circ_{\text{tr},w \to \text{IL}}(\text{C}^+) + \Delta G^\circ_{\text{s,W}} \tag{25}$$

Interestingly, for the ILs composed of the same anion but different cations, the variation of $\Delta G^\circ_{\text{IP-ex}}$ with the kind of C^+ was close to that of $-\Delta G^\circ_{\text{s,W}}$. For example, the variations of $\Delta G^\circ_{\text{IP-ex}}$ from $[\text{OMIm}][\text{NTf}_2]$ to $[\text{BMIm}][\text{NTf}_2]$ are 9.8 and 11.6 kJ·mol^{-1} for 2,4-dinitrophenolate and picrate, respectively; the corresponding variation of $-\Delta G^\circ_{\text{s,W}}$ is 11.4 kJ·mol^{-1}. This fact indicates that the $\Delta G^\circ_{\text{tr},W \to \text{IL}}(\text{T}^-) - \Delta G^\circ_{\text{tr},W \to \text{IL}}(\text{A}^-)$ term in eq 24 is almost constant regardless of the kind of C^+. Similarly, for the ILs composed of the same cation but different anions, the variation of $\Delta G^\circ_{\text{IE-ex}}$ with the kind of A^- was nearly equal to that of $\Delta G^\circ_{\text{s,W}}$. For example, the variations of $\Delta G^\circ_{\text{IE-ex}}$ from $[\text{BMIm}][\text{PF}_6]$ to $[\text{BMIm}][\text{NTf}_2]$ are 7.2, 7.6, and 7.8 kJ·mol^{-1} for 2,4-dinitrophenolate, 2,6-dinitrophenolate, and picrate, respectively; the corresponding variation of $\Delta G^\circ_{\text{s,W}}$ is 7.4 kJ·mol^{-1}. It follows from this that the $\Delta G^\circ_{\text{tr},W \to \text{IL}}(\text{T}^-) + \Delta G^\circ_{\text{tr},W \to \text{IL}}(\text{C}^+)$ term in eq 25 is independent of the kind of A^-. Consequently, it is suggested that the dependence of the extraction equilibrium constants on the IL component ions can be predicted from the dependence of K_{sp}. For a given A^-, the $K_{\text{IP-ex}}$ value varies with the kind of C^+ in inverse proportion to the K_{sp} value. For a given C^+, the $K_{\text{IE-ex}}$ value varies with the kind of A^- in proportion to the K_{sp} value.

To discuss the differences in the extraction equilibrium constants of the different phenolates in a given IL/water system, we examined the relationship between the $\Delta G^\circ_{\text{IP-ex}}$ or $\Delta G^\circ_{\text{IE-ex}}$ value and the standard Gibbs energy of transfer from water to nitrobenzene ($\Delta G^\circ_{\text{tr},W \to \text{NB}}(\text{T}^-)$) for nitrophenolate ions. The $\Delta G^\circ_{\text{tr},W \to \text{NB}}(\text{T}^-)$ values at 298.2 K for 2-nitrophenolate, 3-nitrophenolate, and 4-nitrophenolate were determined in this study to be 21.8 ± 0.3, 24.8 ± 1.2, and 21.8 ± 1.3 kJ·mol^{-1}, respectively (the experimental method is described in the Supporting Information). Literature values of $\Delta G^\circ_{\text{tr},W \to \text{NB}}(\text{T}^-)$ at 298 K were cited for 2,4-dinitrophenolate (7.4 kJ·mol^{-1}), 2,6-dinitrophenolate (8.0 kJ·mol^{-1}), and picrate (-5 kJ·mol^{-1}).[30] All the $\Delta G^\circ_{\text{tr},W \to \text{NB}}(\text{T}^-)$ values are based on the tetraphenylarsonium tetraphenylborate assumption. In Figure 6, the $\Delta G^\circ_{\text{IE-ex}}$ values in the $[\text{BMIm}][\text{PF}_6]$/water and $[\text{OMIm}][\text{BF}_4]$/water systems are plotted against the $\Delta G^\circ_{\text{tr},W \to \text{NB}}(\text{T}^-)$ values. For each biphasic system, a good positive correlation is observed.

Good correlations with $\Delta G^\circ_{\text{tr},W \to \text{NB}}(\text{T}^-)$ were also found for the $\Delta G^\circ_{\text{IP-ex}}$ values. These results indicate that the $\Delta G^\circ_{\text{tr},W \to \text{IL}}(\text{T}^-)$ value in eqs 21 and 22 correlates with the $\Delta G^\circ_{\text{tr},W \to \text{NB}}(\text{T}^-)$ value. Therefore, it appears that in a given IL/water system the difference in extractability of the nitrophenolate anions is mostly governed by that in their hydrophobicity. For some other ions, correlation between the standard Gibbs energy of ion transfer from water to IL and that from water to an organic solvent was reported.[22]

Factors Governing Extraction Power of ILs toward Anion. The D values of a given phenolate anion in different IL/water systems under the condition that $\Delta[\text{T}^-]_\text{W} \ll K_{\text{sp}}^{1/2}$ were compared. The variations of the extractability of $[\text{Pic}^-]$ with the kinds of C^+ and A^- were as follows: $[\text{OMIm}][\text{NTf}_2]$ (1.94) $\gg$ $[\text{BMIm}]-[\text{NTf}_2]$ (0.87) > $[\text{BMPyr}][\text{NTf}_2]$ (0.54);[14] $[\text{OMIm}][\text{BF}_4]$ (3.76)[14] $\gg$ $[\text{OMIm}][\text{NTf}_2]$ (1.94); $[\text{BMIm}][\text{PF}_6]$ (1.56) > $[\text{BMIm}][\text{NTf}_2]$ (0.87), where the values in parentheses are $\log D$ under the above condition. Similar IL dependences were observed for other phenolate ions.[14] It is shown that an IL formed by a more hydrophobic cation and a more hydrophilic anion has a higher extraction power toward the phenolate anions. The dependences of the anion extractability on the kinds of the IL component ions can be explained on the basis of eq 19 or eq 20. For example, the following equation is derived from eq 20.

$$\log D = \log K_{\text{IE-ex}} - (1/2)\log K_{\text{sp}} \tag{26}$$

For a given A^-, the K_{sp} value of the IL decreases with increasing hydrophobicity of C^+, whereas the $K_{\text{IE-ex}}$ value is insensitive to the kind of C^+. Therefore, according to eq 26, the variation of log D with C^+ should be almost equal to that of $-(1/2)\log K_{\text{sp}}$. On the other hand, for a given C^+, both of the K_{sp} and $K_{\text{IE-ex}}$ values decreases with increasing hydrophilicity of A^-. As described in the preceding section, the variation of $\log K_{\text{IE-ex}}$ with the kind of A^- is nearly equal to that of $\log K_{\text{sp}}$. Therefore, according to eq 26, the variation of log D with A^- should be close to that of $(1/2)\log K_{\text{sp}}$. The same conclusion is also reached from eq 19. These theoretical predictions were supported by the experimental results; for example, the variation of log D of $[\text{Pic}]^-$ from the $[\text{BMIm}][\text{NTf}_2]$/water system to the $[\text{OMIm}][\text{NTf}_2]$/water system is 1.07 and the corresponding variation of $-(1/2)\log K_{\text{sp}}$ is 1.00; the variation of log D of $[\text{Pic}]^-$ from the $[\text{BMIm}]-[\text{NTf}_2]$/water system to the $[\text{BMIm}][\text{PF}_6]$/water system is 0.69 and that of $(1/2)\log K_{\text{sp}}$ is 0.65. Therefore, it is suggested as a rule that the distribution ratio varies with the kind of C^+ in inverse proportion to the $K_{\text{sp}}^{1/2}$ value and with the kind of A^- in proportion to the $K_{\text{sp}}^{1/2}$ value.

■ CONCLUSIONS

Through the study of the partition of phenolate anions (T^-), particularly picrate ion, in several IL/water biphasic systems, the following findings were obtained.

(1) From the standpoint of equilibrium, the extraction of T^- from the aqueous phase to the IL one can be accounted for by both the models of ion pair extraction with the IL component cation (C^+) in the aqueous phase and of ion exchange with the IL component anion (A^-) in the IL phase. The aqueous concentrations of C^+ and A^- are governed by the solubility product (K_{sp}) of the IL. The ratio of the equilibrium constant of the ion exchange extraction ($K_{\text{IE-ex}}$) to that of the ion pair extraction ($K_{\text{IP-ex}}$) is always equal to K_{sp}.

858

dx.doi.org/10.1021/jp210444n | *J. Phys. Chem. B* 2012, 116, 852–859

(2) The distribution ratio of T^- is a function of $\Delta[T^-]_W$ ($=[T^-]_W^0 - [T^-]_W$), namely, the amount of decrease of the aqueous concentration of T^- upon extraction into the IL phase. The distribution ratio of T^- is nearly constant when $\Delta[T^-]_W \ll K_{sp}^{1/2}$. The distribution ratio decreases with increasing $\Delta[T^-]_W$ in the higher $\Delta[T^-]_W$ region, and varies in inverse proportion to $\Delta[T^-]_W$ when $\Delta[T^-]_W \gg K_{sp}^{1/2}$.

(3) The contribution of the ion exchange mechanism in the total extraction is equal to that of the ion pair extraction when $\Delta[T^-]_W \ll K_{sp}^{1/2}$. In the higher $\Delta[T^-]_W$ region, the contribution of the former becomes greater.

(4) For a given T^-, the $K_{IE\text{-}ex}$ value varies with the kind of A^- in proportion to the K_{sp} value, but almost independent of the kind of C^+. On the other hand, the $K_{IP\text{-}ex}$ value is insensitive to the kind of A^-, and varies with the kind of C^+ in inverse proportion to the K_{sp} value. For the phenolate anions studied, a linear free energy relationship is found between the ion exchange extraction (or the ion pair extraction) in each IL/water system and the ion transfer from water to nitrobenzene.

(5) The extractability of a given T^-, under the condition that $\Delta[T^-]_W \ll K_{sp}^{1/2}$, is greater for the IL having more hydrophobic C^+ and more hydrophilic A^-. The distribution ratio is inversely proportional to $K_{sp}^{1/2}$ in the variation with C^+, and proportional to $K_{sp}^{1/2}$ in the variation with A^-.

It is clear that the aqueous solubility product of ILs is an important parameter which characterizes the extraction property of the ILs for the phenolate anions. The above findings are expected to be widely applied to other ILs and anions, and also to cations with some modifications.

■ ASSOCIATED CONTENT

ⓢ Supporting Information. The method for determination of standard Gibbs energies of transfer from water to nitrobenzene of 2-nitrophenolate, 3-nitrophenolate, and 4-nitrophenolate ions. This material is available free of charge via the Internet at http://pubs.acs.org.

■ AUTHOR INFORMATION

Corresponding Author
*Tel.: +81-43-290-2781. Fax: +81-43-290-2874. E-mail: katsuta@faculty.chiba-u.jp.

■ ACKNOWLEDGMENT

■ REFERENCES

(1) Plechkova, N. V.; Seddon, K. R. *Chem. Soc. Rev.* **2008**, *37*, 123–150.

(2) Baker, G. A.; Baker, S. N.; Pandey, S.; Bright, F. V. *Analyst* **2005**, *30*, 800–808.

(3) Koel, M. *Crit. Rev. Anal. Chem.* **2005**, *35*, 177–192.

(4) Han, X.; Armstrong, D. W. *Acc. Chem. Res.* **2007**, *40*, 1079–1086.

(5) Liu, R.; Liu, J.-F.; Yin, Y.-G.; Hu, X.-L.; Jiang, G.-B. *Anal. Bioanal. Chem.* **2009**, *393*, 871–883.

(6) Sun, P.; Armstrong, D. W. *Anal. Chim. Acta* **2010**, *661*, 1–16.

(7) Meindersma, G. W.; Podt, A.; Meseguer, M. G.; de Haan, A. B. *ACS Symp. Ser.* **2005**, *902*, 57–71.

(8) Zhao, H.; Xia, S.; Ma, P. *J. Chem. Technol. Biotechnol.* **2005**, *80*, 1089–1096.

(9) Dietz, M. L. *Sep. Sci. Technol.* **2006**, *41*, 2047–2063.

(10) Poole, C. F.; Poole, S. K. *J. Chromatogr. A* **2010**, *1217*, 2268–2286.

(11) Li, Z.; Pei, Y.; Wang, H.; Fan, J.; Wang, J. *Trends Anal. Chem.* **2010**, *29*, 1336–1346.

(12) Billard, I.; Ouadi, A.; Gaillard, C. *Anal. Bioanal. Chem.* **2011**, *400*, 1555–1566.

(13) Abbott, A. P.; Frisch, G.; Hartley, J.; Ryder, K. S. *Green Chem.* **2011**, *13*, 471–481.

(14) Katsuta, S.; Nakamura, K.; Kudo, Y.; Takeda, Y.; Kato, H. *J. Chem. Eng. Data* **2011**, *56*, 4083–4089.

(15) Dietz, M. L.; Dzielawa, J. A. *Chem. Commun.* **2001**, 2124–2125.

(16) Shimojo, K.; Goto, M. *Anal. Chem.* **2004**, *76*, 5039–5044.

(17) Dietz, M. L.; Dzielawa, J. A.; Jensen, M. P.; Beitz, J. V.; Borkowski, M. *ACS Symp. Ser.* **2005**, *902*, 2–18.

(18) Li, C.; Xin, B.; Xu, W.; Zhang, Q. *J. Chem. Technol. Biotechnol.* **2007**, *82*, 196–204.

(19) Kozonoi, N.; Ikeda, Y. *Monatsh. Chem.* **2007**, *138*, 1145–1151.

(20) Chaumont, A.; Wipff, G. *J. Phys. Chem. B* **2010**, *114*, 13773–13785.

(21) Nishi, N.; Imakura, S.; Kakiuchi, T. *Anal. Chem.* **2006**, *78*, 2726–2731.

(22) Langmaier, J.; Samec, Z. *Electrochem. Commun.* **2007**, *9*, 2633–2638.

(23) Samec, Z.; Langmaier, J.; Kakiuchi, T. *Pure Appl. Chem.* **2009**, *81*, 1473–1488.

(24) Nakamura, K.; Kudo, Y.; Takeda, Y.; Katsuta, S. *J. Chem. Eng. Data* **2011**, *56*, 2160–2167.

(25) Freire, M. G.; Carvalho, P. J.; Gardas, R. L.; Marrucho, I. M.; Santos, L. M. N. B. F.; Coutinho, J. A. P. *J. Phys. Chem. B* **2008**, *112*, 1604–1610.

(26) Freire, M. G.; Neves, C. M. S. S.; Carvalho, P. J.; Gardas, R. L.; Fernandes, A. M.; Marrucho, I. M.; Santos, L. M. N. B. F.; Coutinho, J. A. P. *J. Phys. Chem. B* **2007**, *111*, 13082–13089.

(27) Anthony, J. L.; Maginn, E. J.; Brennecke, J. F. *J. Phys. Chem. B* **2001**, *105*, 10942–10949.

(28) Hirohata, Y.; Nishi, N.; Kakiuchi, T. *J. Chem. Eng. Data* **2010**, *55*, 1980–1985.

(29) Katsuta, S.; Ogawa, R.; Yamaguchi, N.; Ishitani, T.; Takeda, Y. *J. Chem. Eng. Data* **2007**, *52*, 248–251.

(30) Rais, J. *Collect. Czech. Chem. Commun.* **1971**, *36*, 3253–3262.

859

dx.doi.org/10.1021/jp210444n |*J. Phys. Chem. B* 2012, 116, 852–859